

A Critical Analysis of Computational and Imaging Methods for Epileptogenic Lesion Detection

Yusuf Qwareeq

Department of Electrical and Computer Engineering
Temple University

June 27, 2025

A presentation for the defense of the preliminary examination.

Presentation Outline

- 1 The Clinical Imperative
- 2 A Narrative of Scientific Progress
- 3 Act I: The Foundational Problem and Early Solution
- 4 Act II: The Paradigm-Shifting Tool
- 5 Act III: The Modern Synthesis
- 6 Synthesis, Discussion, and Conclusion

The Challenge of Drug-Resistant Epilepsy (DRE)

Epilepsy is a Prevalent Neurological Disorder

- Affects millions of people worldwide.
- Up to one-third of patients develop **Drug-Resistant Epilepsy (DRE)**: failure of two tolerated and appropriate anti-seizure medications [1].
- Pooled prevalence of DRE is **36.3%** in clinic-based cohorts [2].

The Challenge of Drug-Resistant Epilepsy (DRE)

Epilepsy is a Prevalent Neurological Disorder

- Affects millions of people worldwide.
- Up to one-third of patients develop **DRE**: failure of two tolerated and appropriate anti-seizure medications [1].
- Pooled prevalence of DRE is **36.3%** in clinic-based cohorts [2].

Surgery: The Best Hope for Focal DRE

- For focal epilepsy, resective surgery offers the best path to seizure freedom.
- Seizure-free rates: **57.0%** (surgical group) vs. **15.3%** (medical group) [3].



Figure: Temporal-lobe resection under an operating microscope, illustrating surgical treatment for focal DRE (photo: Mansi Agrawal, CC-BY-SA 4.0).

The Surgical Prerequisite: Finding the Epileptogenic Zone

The Central Problem

Surgical success is critically dependent on the accurate presurgical localization of the **Epileptogenic Zone (EZ)**: the area of cortex indispensable for generating seizures.

The Surgical Prerequisite: Finding the Epileptogenic Zone

The Central Problem

Surgical success is critically dependent on the accurate presurgical localization of the **EZ**: the area of cortex indispensable for generating seizures.

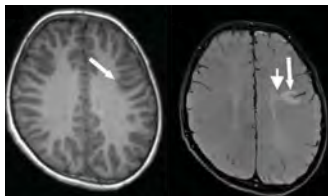


Figure: Routine axial MRI (left) appears normal, whereas FLAIR (right) reveals a subtle FCD (photo: Kusama et al., *Neurology: Clinical Practice* 2021, CC BY 4.0).

“MRI-Negative” Epilepsy

- **15% to 40%** of focal DRE patients are classified as “MRI-negative” [4].
- Routine radiological review of structural MRI fails to identify a clear lesion.
- This is a primary negative prognostic indicator for surgery [5].
- Most common underlying cause: **FCD Type II**, a subtle malformation of cortical development.

The Surgical Prerequisite: Finding the Epileptogenic Zone

The Central Problem

Surgical success is critically dependent on the accurate presurgical localization of the **EZ**: the area of cortex indispensable for generating seizures.

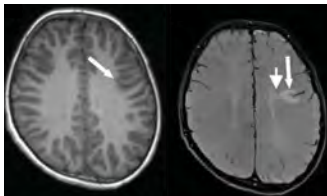


Figure: Routine axial MRI (left) appears normal, whereas FLAIR (right) reveals a subtle FCD (photo: Kusama et al., *Neurology: Clinical Practice* 2021, CC BY 4.0).

“MRI-Negative” Epilepsy

- **15% to 40%** of focal DRE patients are classified as “MRI-negative” [4].
- Routine radiological review of structural MRI fails to identify a clear lesion.
- This is a primary negative prognostic indicator for surgery [5].
- Most common underlying cause: **FCD Type II**, a subtle malformation of cortical development.

The Imperative

We urgently need better imaging and computation to reveal hidden lesions [6].

Tracing a Path of Innovation: A Three-Act Narrative

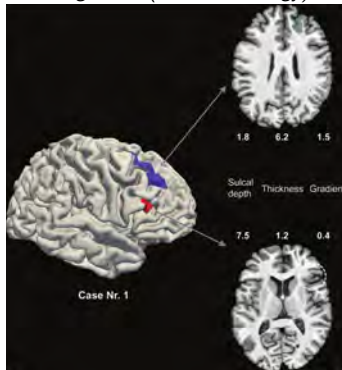
This analysis argues that progress in this field has followed a cohesive narrative arc, characterized by the identification of a problem, the invention of an enabling technology, and their ultimate synthesis into a modern solution.

Tracing a Path of Innovation: A Three-Act Narrative

This analysis argues that progress in this field has followed a cohesive narrative arc, characterized by the identification of a problem, the invention of an enabling technology, and their ultimate synthesis into a modern solution.

Act I: Problem Definition

Hong et al. (2014, Neurology)



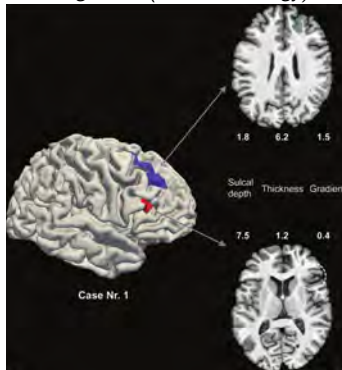
Defining the problem with classical ML on clinical MRI.

Tracing a Path of Innovation: A Three-Act Narrative

This analysis argues that progress in this field has followed a cohesive narrative arc, characterized by the identification of a problem, the invention of an enabling technology, and their ultimate synthesis into a modern solution.

Act I: Problem Definition

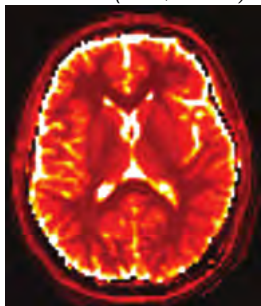
Hong et al. (2014, Neurology)



Defining the problem with classical ML on clinical MRI.

Act II: Tool Invention

Ma et al. (2013, Nature)



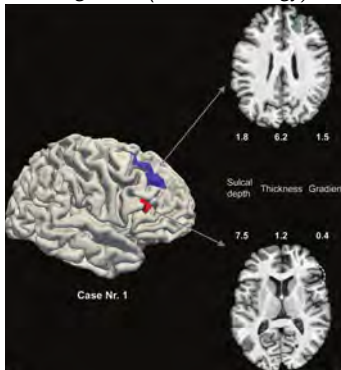
Inventing a new tool for rapid, quantitative imaging.

Tracing a Path of Innovation: A Three-Act Narrative

This analysis argues that progress in this field has followed a cohesive narrative arc, characterized by the identification of a problem, the invention of an enabling technology, and their ultimate synthesis into a modern solution.

Act I: Problem Definition

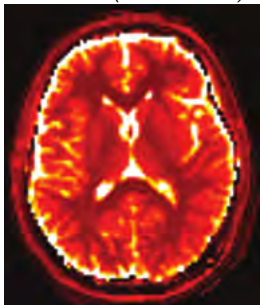
Hong et al. (2014, Neurology)



Defining the problem with classical ML on clinical MRI.

Act II: Tool Invention

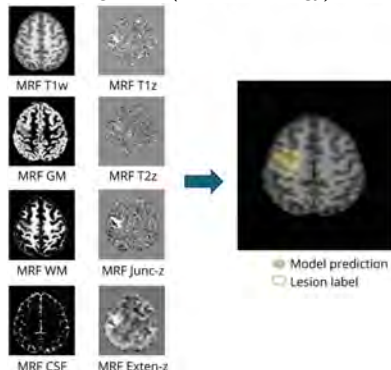
Ma et al. (2013, Nature)



Inventing a new tool for rapid, quantitative imaging.

Act III: Modern Synthesis

Ding et al. (2025, Neurology)



Synthesizing tool and problem with DL for superior detection.

Act I: Hong et al. (2014) - Automated Detection of FCD Type II [7]

Research Objective

To develop and validate a **fully automated method** to detect FCD Type II lesions in MRI-negative patients using conventional T_1 -Weighted (T1w) MRI scans.

Act I: Hong et al. (2014) - Automated Detection of FCD Type II [7]

Research Objective

To develop and validate a **fully automated method** to detect FCD Type II lesions in MRI-negative patients using conventional T1w MRI scans.

Key Innovation

Shift the paradigm from computer-aided *visualization* (requiring expert interpretation) to computer-aided *detection* (providing an objective classification).

Act I: Hong et al. (2014) - Automated Detection of FCD Type II [7]

Research Objective

To develop and validate a **fully automated method** to detect FCD Type II lesions in MRI-negative patients using conventional T1w MRI scans.

Key Innovation

Shift the paradigm from computer-aided *visualization* (requiring expert interpretation) to computer-aided *detection* (providing an objective classification).

Table: Patient cohorts used in the study by Hong et al. (2014).

Group (N)	Description
Primary Dataset (3.0 T, 1.0 mm isotropic T1w)	
Patients (19)	MRI-negative with histopathologically confirmed FCD Type II
Healthy Controls (24)	No history of neurological or psychiatric disease
Disease Controls (11)	Seizure-free post-op for non-lesional TLE
Validation Dataset (1.5 T, 1.0 mm isotropic T1w)	
Patients (14)	MRI-negative with histopathologically confirmed FCD
Healthy Controls (20)	Matched to patient group

Hong et al. Methodology: Handcrafted Features

The core of the method lies in extracting five biologically-informed, handcrafted features from a cortical surface model derived from T1w MRI.

Hong et al. Methodology: Handcrafted Features

The core of the method lies in extracting five biologically-informed, handcrafted features from a cortical surface model derived from T1w MRI.

- 1 **Cortical Thickness:** *Models cortical thickening common in FCD.*

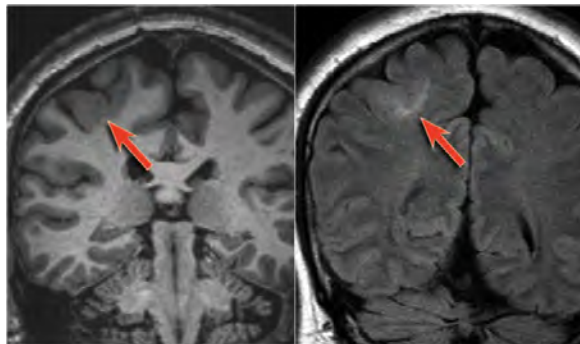


Figure: T1w MRI (left) shows cortical thickening and GM-WM blurring, while FLAIR (right) reveals matching subcortical hyperintensity, typical of FCD Type II (photo: © RadiologyAssistant.nl, educational reuse).

Hong et al. Methodology: Handcrafted Features

The core of the method lies in extracting five biologically-informed, handcrafted features from a cortical surface model derived from T1w MRI.

- 1 **Cortical Thickness:** *Models cortical thickening common in FCD.*
- 2 **Sulcal Depth:** *Captures lesions at the bottom of abnormally deep sulci.*

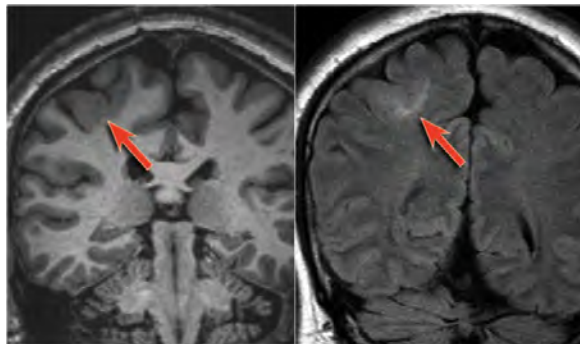


Figure: T1w MRI (left) shows cortical thickening and GM-WM blurring, while FLAIR (right) reveals matching subcortical hyperintensity, typical of FCD Type II (photo: © RadiologyAssistant.nl, educational reuse).

Hong et al. Methodology: Handcrafted Features

The core of the method lies in extracting five biologically-informed, handcrafted features from a cortical surface model derived from T1w MRI.

- ❶ **Cortical Thickness:** *Models cortical thickening common in FCD.*
- ❷ **Sulcal Depth:** *Captures lesions at the bottom of abnormally deep sulci.*
- ❸ **Mean Curvature:** *Models local changes in cortical folding patterns.*

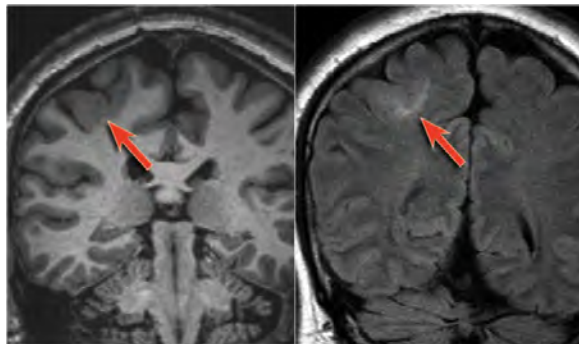


Figure: T1w MRI (left) shows cortical thickening and GM-WM blurring, while FLAIR (right) reveals matching subcortical hyperintensity, typical of FCD Type II (photo: © RadiologyAssistant.nl, educational reuse).

Hong et al. Methodology: Handcrafted Features

The core of the method lies in extracting five biologically-informed, handcrafted features from a cortical surface model derived from T1w MRI.

- ❶ **Cortical Thickness:** *Models cortical thickening common in FCD.*
- ❷ **Sulcal Depth:** *Captures lesions at the bottom of abnormally deep sulci.*
- ❸ **Mean Curvature:** *Models local changes in cortical folding patterns.*
- ❹ **Relative Intensity:** *Quantifies T_1 signal hyperintensity in the cortical ribbon.*

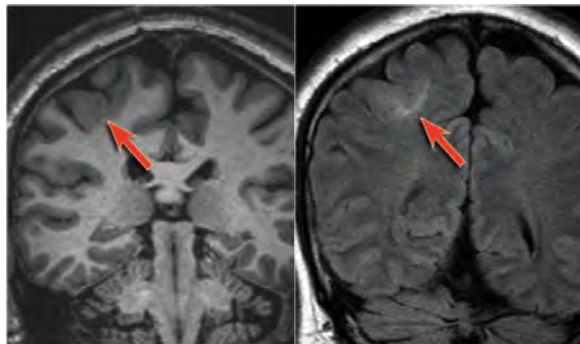


Figure: T1w MRI (left) shows cortical thickening and GM-WM blurring, while FLAIR (right) reveals matching subcortical hyperintensity, typical of FCD Type II (photo: © RadiologyAssistant.nl, educational reuse).

Hong et al. Methodology: Handcrafted Features

The core of the method lies in extracting five biologically-informed, handcrafted features from a cortical surface model derived from T1w MRI.

- ❶ **Cortical Thickness:** *Models cortical thickening common in FCD.*
- ❷ **Sulcal Depth:** *Captures lesions at the bottom of abnormally deep sulci.*
- ❸ **Mean Curvature:** *Models local changes in cortical folding patterns.*
- ❹ **Relative Intensity:** *Quantifies T_1 signal hyperintensity in the cortical ribbon.*
- ❺ **Intensity Gradient:** *A proxy for the blurring of the GM-WM junction.*

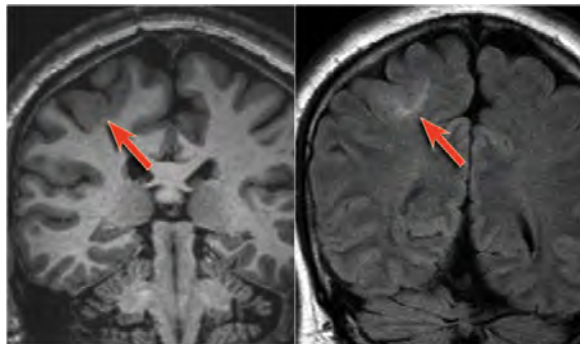


Figure: T1w MRI (left) shows cortical thickening and GM-WM blurring, while FLAIR (right) reveals matching subcortical hyperintensity, typical of FCD Type II (photo: © RadiologyAssistant.nl, educational reuse).

Hong et al. Methodology: A Two-Stage Classifier

This architecture is an engineered solution to the **massive multiple comparisons problem** inherent in whole-brain, vertex-wise analysis.

Stage 1: Vertex-wise Classification

- An Linear Discriminant Analysis (LDA) classifies each individual vertex ($>80,000$ per brain) as “lesional” or “non-lesional” based on the 5-feature vector.
- **Result:** High sensitivity, but an extremely high number of false-positives due to noise.

Hong et al. Methodology: A Two-Stage Classifier

This architecture is an engineered solution to the **massive multiple comparisons problem** inherent in whole-brain, vertex-wise analysis.

Stage 1: Vertex-wise Classification

- An LDA classifies each individual vertex ($>80,000$ per brain) as “lesional” or “non-lesional” based on the 5-feature vector.
- **Result:** High sensitivity, but an extremely high number of false-positives due to noise.



Stage 2: Cluster-wise Classification (The Innovation)

- A second LDA classifies *entire clusters* of abnormal vertices from Stage 1.
- **Input:** Statistical moments of each cluster (mean, std, skew, kurtosis of features).
- **Goal:** Learns the multivariate profile of a true lesion, distinguishing it from noise.

Hong et al. Key Findings

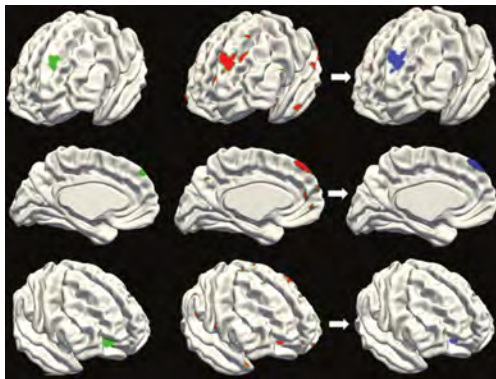


Figure: Surface projections for three MRI-negative patients. Manual lesion labels are shown in green, vertex-wise classification highlights multiple candidates in red, and cluster-wise refinement removes false positives, leaving only the cluster that aligns with the manual label in blue.

Hong et al. Key Findings

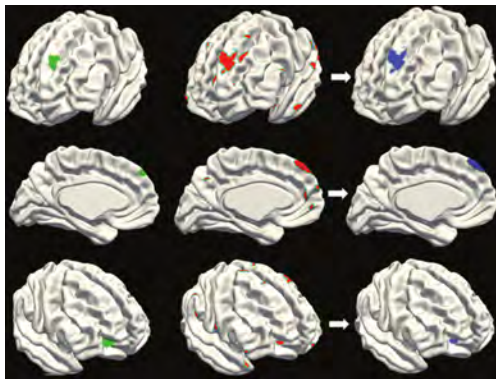


Figure: Surface projections for three MRI-negative patients. Manual lesion labels are shown in green, vertex-wise classification highlights multiple candidates in red, and cluster-wise refinement removes false positives, leaving only the cluster that aligns with the manual label in blue.

Table: Classifier performance on the two datasets. Values in parentheses represent 95% CIs.

	Primary (3.0 T)	Validation (1.5 T)
Sensitivity	74% (54-94%)	71% (48-94%)
Specificity	100% (91-100%)	95% (85-100%)

Hong et al. Key Findings

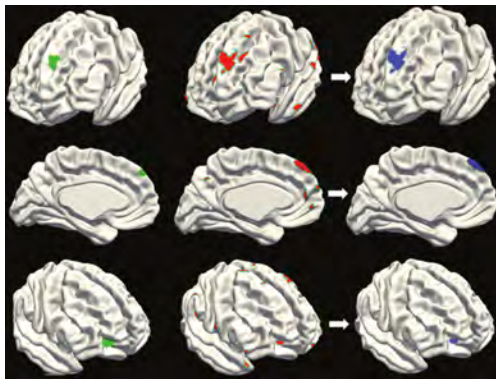


Figure: Surface projections for three MRI-negative patients. Manual lesion labels are shown in green, vertex-wise classification highlights multiple candidates in red, and cluster-wise refinement removes false positives, leaving only the cluster that aligns with the manual label in blue.

Table: Classifier performance on the two datasets. Values in parentheses represent 95% CIs.

	Primary (3.0 T)	Validation (1.5 T)
Sensitivity	74% (54-94%)	71% (48-94%)
Specificity	100% (91-100%)	95% (85-100%)

A Key Clinical Caveat

In **50%** of true-positive cases, additional “extralesional” clusters also appeared, creating potential clinical ambiguity.

Act I: Critical Appraisal

Strengths and Contributions

- **Powerful Proof-of-Concept (PoC):** Showed that an algorithm could automatically detect lesions invisible to the human eye.
- **Forced a Paradigm Shift:** Argued that “MRI-negative” is a technological limitation, not a biological diagnosis.
- **Clinical Utility:** Provided an objective, data-driven tool to generate surgical hypotheses.

Act I: Critical Appraisal

Strengths and Contributions

- **Powerful PoC:** Showed that an algorithm could automatically detect lesions invisible to the human eye.
- **Forced a Paradigm Shift:** Argued that “MRI-negative” is a technological limitation, not a biological diagnosis.
- **Clinical Utility:** Provided an objective, data-driven tool to generate surgical hypotheses.

Limitations and Path Forward

- **Low Statistical Power:** The small sample size ($N=19$) results in very wide confidence intervals for sensitivity (e.g., 54-94%), indicating major uncertainty in the true performance.
- **Validation Method:** LOOCV was necessary for the small N but can have high variance; the classifier itself is a heuristic, not a formal statistical test.
- **Spectrum Bias:** The cohort was pre-selected, not a random sample, which likely inflates reported performance.
- **Clinical Ambiguity:** Extralesional clusters in 50% of true positives limit diagnostic certainty.
- **Data-Limited:** The classifier is constrained by a single, qualitative T1w image, motivating the need for richer data acquisition.
- **Model-Limited:** The method's success is bound by 5 handcrafted features, motivating a shift to more powerful models.

Act I: Critical Appraisal

Strengths and Contributions

- **Powerful PoC:** Showed that an algorithm could automatically detect lesions invisible to the human eye.
- **Forced a Paradigm Shift:** Argued that “MRI-negative” is a technological limitation, not a biological diagnosis.
- **Clinical Utility:** Provided an objective, data-driven tool to generate surgical hypotheses.

Limitations and Path Forward

- **Low Statistical Power:** The small sample size ($N=19$) results in very wide confidence intervals for sensitivity (e.g., 54-94%), indicating major uncertainty in the true performance.
- **Validation Method:** LOOCV was necessary for the small N but can have high variance; the classifier itself is a heuristic, not a formal statistical test.
- **Spectrum Bias:** The cohort was pre-selected, not a random sample, which likely inflates reported performance.
- **Clinical Ambiguity:** Extralesional clusters in 50% of true positives limit diagnostic certainty.
- **Data-Limited:** The classifier is constrained by a single, qualitative T1w image, motivating the need for richer data acquisition.
- **Model-Limited:** The method's success is bound by 5 handcrafted features, motivating a shift to more powerful models.

These limitations clearly define the next steps needed: a better imaging tool and a more powerful analytical model.

Act II: Ma et al. (2013) - Magnetic Resonance Fingerprinting (MRF) [8]

Research Objective

To overcome the limitations of conventional MRI by inventing a new framework for **rapid, simultaneous, and quantitative** measurement of multiple tissue properties from a single acquisition.

Act II: Ma et al. (2013) - Magnetic Resonance Fingerprinting (MRF) [8]

Research Objective

To overcome the limitations of conventional MRI by inventing a new framework for **rapid, simultaneous, and quantitative** measurement of multiple tissue properties from a single acquisition.

Table: A comparison of MRI paradigms, highlighting the MRF innovation.

	Conventional Qualitative	Conventional Quantitative	Magnetic Resonance Fingerprinting
Primary Output	Weighted images with arbitrary units (a.u.)	Single quantitative map per scan	Multiple, simultaneous quantitative maps
Acquisition	Steady-state signal	Multiple steady-state scans	Single, non-steady-state scan
Scan Time	Fast per contrast	Slow and time-prohibitive per parameter	Very fast for all parameters
Robustness	Low to artifacts and motion	Low to patient motion and errors	High to artifacts and motion

Act II: Ma et al. (2013) - Magnetic Resonance Fingerprinting (MRF) [8]

Research Objective

To overcome the limitations of conventional MRI by inventing a new framework for **rapid, simultaneous, and quantitative** measurement of multiple tissue properties from a single acquisition.

Table: A comparison of MRI paradigms, highlighting the MRF innovation.

	Conventional Qualitative	Conventional Quantitative	Magnetic Resonance Fingerprinting
Primary Output	Weighted images with arbitrary units (a.u.)	Single quantitative map per scan	Multiple, simultaneous quantitative maps
Acquisition	Steady-state signal	Multiple steady-state scans	Single, non-steady-state scan
Scan Time	Fast per contrast	Slow and time-prohibitive per parameter	Very fast for all parameters
Robustness	Low to artifacts and motion	Low to patient motion and errors	High to artifacts and motion

The Conceptual Leap

MRF is not just an incremental improvement; it is a fundamental reimaging of the entire MR experiment. It is a foundational, “tool-building” technology.

MRF Methodology: A Three-Step Process

1. Create Fingerprints 2. Build Dictionary 3. Match and Quantify

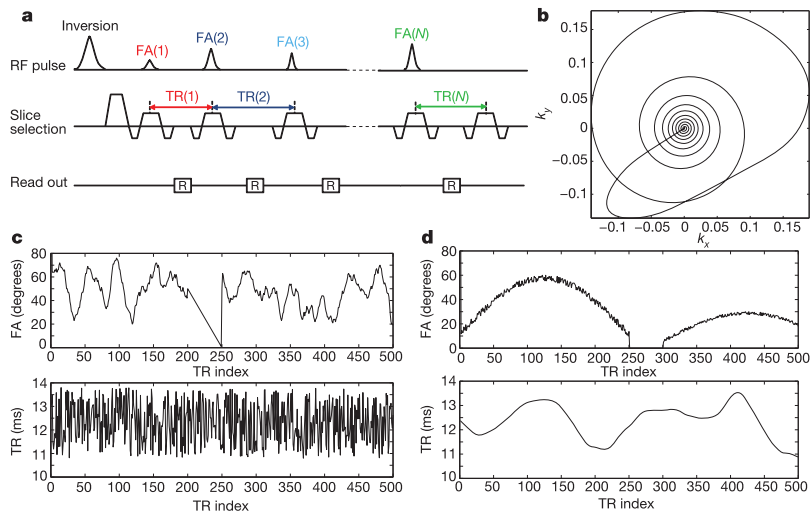


Figure: A sequence with pseudorandomly varying parameters (e.g., Flip Angle (FA), Repetition Time (TR)) creates a unique, non-steady-state signal evolution for each tissue type – its “fingerprint.”

MRF Methodology: A Three-Step Process

1. Create Fingerprints
2. Build Dictionary
3. Match and Quantify

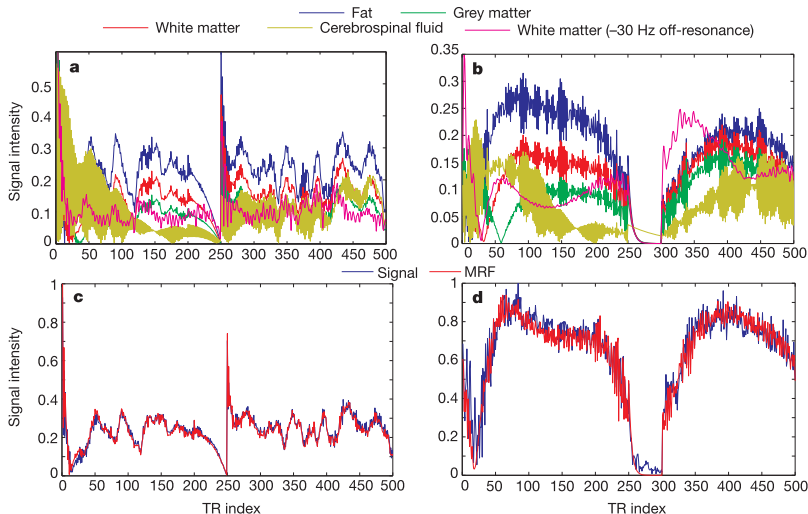


Figure: A massive dictionary is pre-computed by simulating the Bloch equations for a vast range of tissue properties (T_1 , T_2), using the exact same sequence parameters from Step 1.

MRF Methodology: A Three-Step Process

1. Create Fingerprints
2. Build Dictionary
3. Match and Quantify

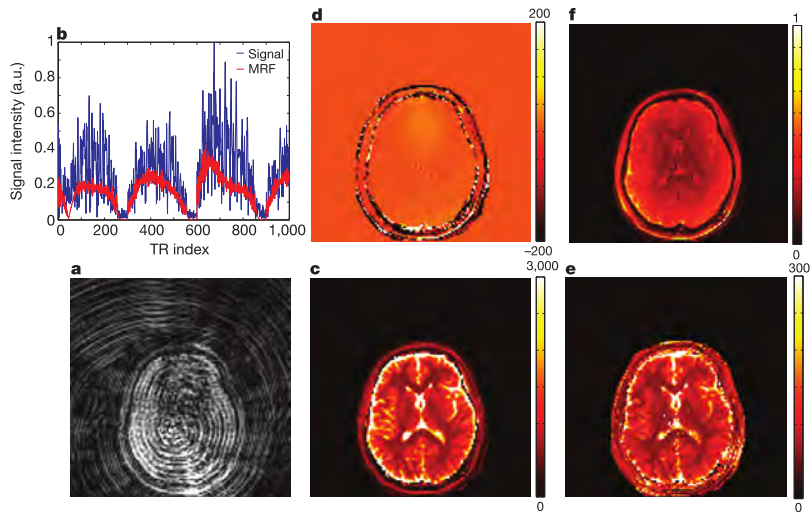


Figure: The measured fingerprint from each voxel is matched to the best-fitting dictionary entry via normalized dot product. Incoherent aliasing artifacts are inherently rejected.

Ma et al. Key Findings: A Robust and Accurate Technology

Efficiency and Robustness

- Generates multiple co-registered quantitative maps from a single scan of ~ 12 s per slice.
- Extremely robust to undersampling artifacts and bulk patient motion.

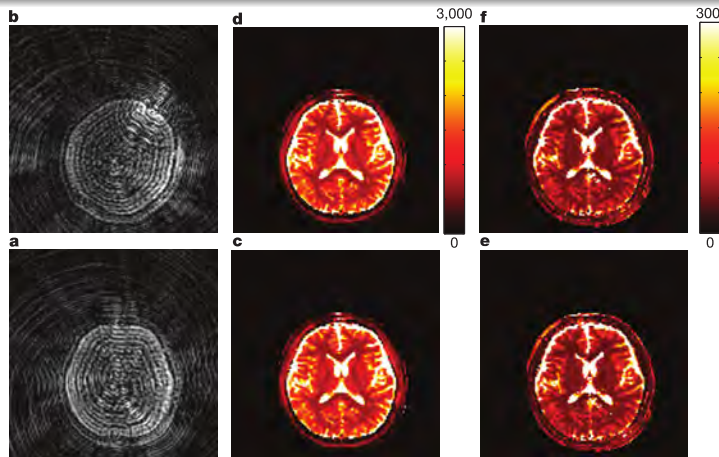


Figure: Motion-corrupted scans yield nearly identical quantitative maps (Concordance Correlation Coefficient (CCC) >0.97 after ± 5 mm motion).

Ma et al. Key Findings: A A Robust and Accurate Technology

Accuracy and Precision

- MRF measurements show excellent agreement with gold-standard methods.
- CCC of **0.988** for T_1 and **0.974** for T_2 .
- High repeatability (precision) over time.

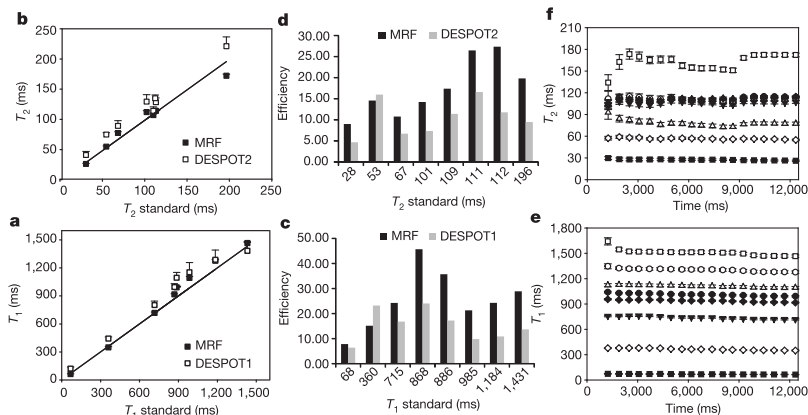


Figure: High correlation with standard methods (a, b) and high precision (e, f).

Act II: Critical Appraisal

Strengths and Contributions

- **A Philosophical Shift:** Moved MRI from a qualitative art to a quantitative science. The output is now objective, reproducible physical constants.
- **The Ultimate Enabling Technology:** MRF provides the ideal raw material for advanced computational analysis: rich, multiparametric, quantitative, and perfectly co-registered data.

Act II: Critical Appraisal

Strengths and Contributions

- **A Philosophical Shift:** Moved MRI from a qualitative art to a quantitative science. The output is now objective, reproducible physical constants.
- **The Ultimate Enabling Technology:** MRF provides the ideal raw material for advanced computational analysis: rich, multiparametric, quantitative, and perfectly co-registered data.

Limitation (Within This Narrative)

- The paper by Ma et al. is a work of foundational physics and engineering. It invents the tool but does not apply it to solve a specific, challenging clinical problem.

Act II: Critical Appraisal

Strengths and Contributions

- **A Philosophical Shift:** Moved MRI from a qualitative art to a quantitative science. The output is now objective, reproducible physical constants.
- **The Ultimate Enabling Technology:** MRF provides the ideal raw material for advanced computational analysis: rich, multiparametric, quantitative, and perfectly co-registered data.

Limitation (Within This Narrative)

- The paper by Ma et al. is a work of foundational physics and engineering. It invents the tool but does not apply it to solve a specific, challenging clinical problem.

Ma et al. provided a powerful new instrument. This created the opportunity for the final act: using this instrument to solve the clinical problem defined in Act I.

Act III: Ding et al. (2025) - The Synthesis of MRF and DL [9]

Research Objective

To develop an **MRF-based DL framework** for whole-brain FCD detection, leveraging quantitative imaging to improve sensitivity and specificity, particularly for the most subtle lesion types.

Act III: Ding et al. (2025) - The Synthesis of MRF and DL [9]

Research Objective

To develop an **MRF-based DL framework** for whole-brain FCD detection, leveraging quantitative imaging to improve sensitivity and specificity, particularly for the most subtle lesion types.

This work represents the culmination of the narrative:

- It addresses the **clinical problem** from Hong et al. (detecting subtle FCD).
- It uses the **advanced tool** from Ma et al. (MRF) to acquire superior data.
- It applies a **modern algorithm** (DL) that overcomes the limitations of classical ML.

The Key Advance: From Feature Engineering to Representation Learning

Instead of using a few pre-defined, handcrafted features, a CNN learns the optimal discriminative features automatically and directly from the rich image data itself.

1. The Data: Rich and Multiparametric

- **Acquisition:** Single ~ 12 min 3D MRF scan at **1.0 mm^3 isotropic resolution**.
- **Input Maps:** Quantitative T_1/T_2 relaxation time (T_2), tissue fractions, and morphometric z-scores.
- **Cohort:** 40 patients with diverse FCD subtypes and 67 healthy controls.

2. The Model: Deep Learning

- **Architecture:** A **3D no-new-U-Net (nnU-Net)** that processes data volumetrically.
- **Training Input:** Supervised learning on **$128 \times 160 \times 112$ -voxel 3D patches**.
- **Validation:** Assessed with a robust patient-level LOOCV scheme.

The key advantage is the richness of the input data, as shown on the next slide...

Framework Component: Multiparametric Input Maps

The Power of Quantitative Data

Note how different maps highlight different aspects of the pathology. This rich, multiparametric view provides a far more informative substrate for a DL model than a single qualitative image.

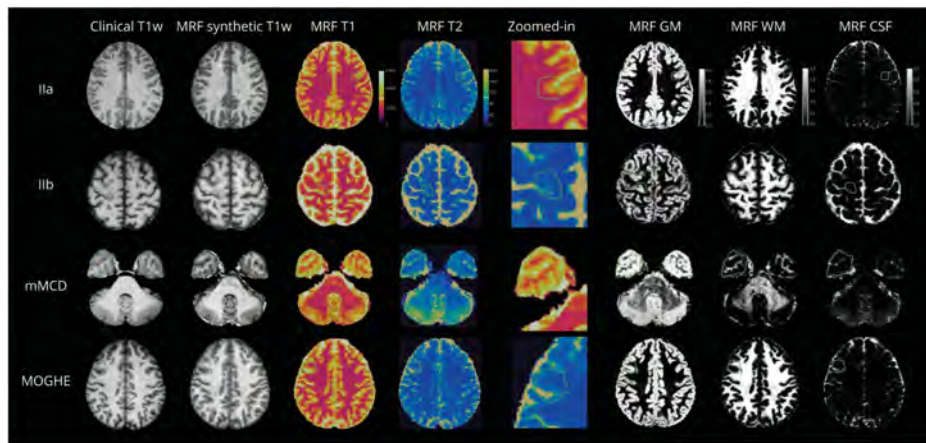


Figure: A single MRF scan provides multiple quantitative views of the same lesion across four different FCD subtypes.

The DL Framework: nnU-Net

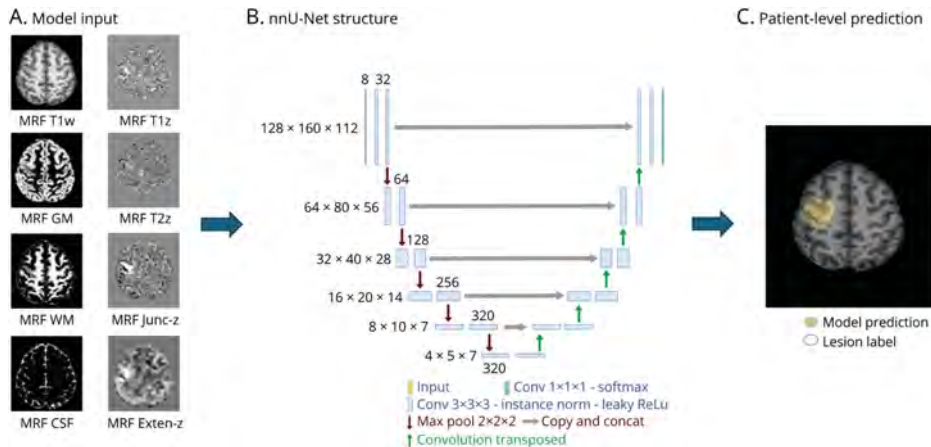
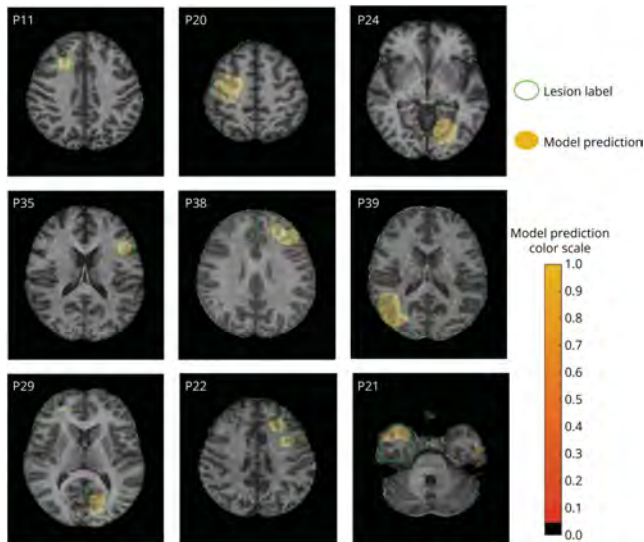


Figure: The integrated workflow. A) Multiparametric maps from one MRF scan serve as input. B) The U-Shaped Convolutional Network (U-Net) CNN processes the data, learning features at multiple scales. C) The model outputs a probabilistic lesion map.

Why U-Net?

The U-Net's encoder-decoder architecture with "skip connections" is ideal for segmentation. It allows the model to combine deep, abstract, contextual information (what the lesion is) with fine-grained, spatial detail (where the lesion is).

Ding et al. Key Findings: State-of-the-Art Performance



High Sensitivity with Low False Positives (FPs)

The final MRF-DL framework achieved:

- Patient-level sensitivity: **80%** (32/40).
- Clinically acceptable FP rate: **1.7 clusters/patient**.

Crucial Benchmark Comparisons

The MRF-DL model dramatically outperformed benchmarks:

- **vs. T1w + DL:** 70% sens., 9.7 FPs/patient. Proves value of **MRF data**.
- **vs. MAP18:** 50% sens., 4.6 FPs/patient. Proves value of **DL model**.

Figure: Examples of successful automated detections. The model's prediction (yellow) accurately localizes the ground-truth lesion (green).

Act III: Critical Appraisal

Strengths and Contributions

- **A Powerful Synthesis:** Successfully integrates a state-of-the-art imaging modality (MRF) with a state-of-the-art analytical model (DL).
- **Superior Performance:** Demonstrates a clear step-change in capability over prior methods, including the one from Hong et al.
- **High Clinical Relevance:** High sensitivity across heterogeneous lesion types with a manageable false-positive rate.

Act III: Critical Appraisal

Strengths and Contributions

- **A Powerful Synthesis:** Successfully integrates a state-of-the-art imaging modality (MRF) with a state-of-the-art analytical model (DL).
- **Superior Performance:** Demonstrates a clear step-change in capability over prior methods, including the one from Hong et al.
- **High Clinical Relevance:** High sensitivity across heterogeneous lesion types with a manageable false-positive rate.

Limitations and Next Steps

- **Lack of External Validation:** The model was developed and tested on data from a single institution. Its generalizability is unproven.
- **The “Black Box” Problem:** The DL model provides a prediction but no explicit reasoning. This is a significant barrier to clinical trust and adoption.

The Evolutionary Trajectory Summarized

This narrative reveals a repeatable “Problem-Tool-Algorithm” paradigm for innovation in computational medicine [10].

Table: A comparative summary of the three cornerstone papers.

Methodology	Hong et al. (2014)	Ma et al. (2013)	Ding et al. (2025)
Role in Narrative	The Problem	The Tool	The Solution
Primary Goal	Detect MRI-negative FCD II	Introduce MRF framework	Detect heterogeneous FCDs
Imaging Modality	Qualitative T1w MRI	Quantitative MRF (PoC)	Quantitative 3D MRF
Feature Engineering	Handcrafted, surface-based	N/A	Automated via DL
Analysis Model	Classical ML (LDA)	Dictionary matching	DL (nnU-Net)
Key Strength	First automated method	Simultaneous quantification	High sensitivity, low FP rate
Key Limitation	Brittle features, simple data	No clinical application	Single-center, “black-box”

Future Directions: Immediate Next Steps

1. Rigorous External Validation

- A large-scale, multicenter study is essential to prove the framework's generalizability and robustness across different scanners, protocols, and patient populations.
- This is a prerequisite for clinical translation and regulatory approval [11, 12].

2. Opening the “Black Box”

- Clinicians are rightly hesitant to trust an algorithm that cannot explain its reasoning [13, 14].
- We must move toward **Explainable Artificial Intelligence (XAI)**:
 - ▶ Creating saliency maps to show which pixels/features drove the decision.
 - ▶ Building more transparent models.
 - ▶ Answering *why* the model flagged a region [15].

Future Directions: XAI in Practice

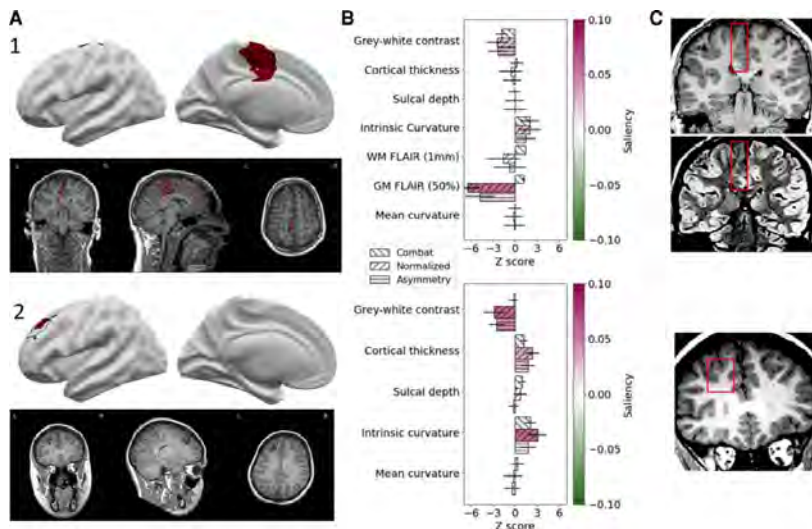


Figure: An XAI model explains its lesion detection (A) by generating saliency maps that visualize which features (B) and voxels (C) were most influential (photo: Spitzer et al., *Brain* 2022, CC BY 4.0).

Future Directions: The Next Frontier

Moving from Localization to Biological Characterization

The ultimate goal is not just to answer “Where is the lesion?” but to understand the molecular and genetic nature of the epileptogenic network.

This requires a multi-modal systems-level approach:

- **Integrate Data Modalities:** Create AI models that fuse data from [16]:
 - ▶ Non-invasive imaging (MRF, Positron Emission Tomography (PET))
 - ▶ Electrophysiology (Stereoelectroencephalography (SEEG), Magnetoencephalography (MEG))
 - ▶ Genomics and transcriptomics
- **Personalized Brain Modeling:** Use this integrated data to inform personalized computational models (“virtual brains”) of a patient’s epilepsy [17].
- **Precision Medicine:** This is the path toward true precision medicine – predicting surgical outcomes, simulating interventions, and discovering novel therapeutic targets.

Conclusion

- This work has traced the evolution of computational methods for detecting epileptogenic lesions, confronting a major challenge in clinical epileptology.
- A clear narrative arc emerged, following a “**Problem-Tool-Algorithm**” paradigm:
 - ① **Hong et al.** established the problem and a PoC solution, highlighting the need for better data.
 - ② **Ma et al.** invented the enabling tool (MRF) that provided this rich, quantitative data.
 - ③ **Ding et al.** synthesized these threads, using a modern algorithm (DL) to leverage the advanced tool and solve the clinical problem with state-of-the-art performance.
- The future of precision epileptology lies in the powerful, iterative, and symbiotic cycle between our ability to **visualize** the brain’s structure with ever-increasing fidelity and our capacity to **model** its complex dynamics [18].

List of Acronyms I

CCC Concordance Correlation Coefficient.

CI Confidence Interval.

CNN Convolutional Neural Network.

DL Deep Learning.

DRE Drug-Resistant Epilepsy.

EZ Epileptogenic Zone.

FA Flip Angle.

FCD Focal Cortical Dysplasia.

FLAIR Fluid Attenuated Inversion Recovery.

FP False Positive.

GM Gray Matter.

List of Acronyms II

LDA Linear Discriminant Analysis.

LOOCV Leave-One-Out Cross-Validation.

MEG Magnetoencephalography.

ML Machine Learning.

MRF Magnetic Resonance Fingerprinting.

MRI Magnetic Resonance Imaging.

nnU-Net no-new-U-Net.

PET Positron Emission Tomography.

PoC Proof-of-Concept.

SEEG Stereoelectroencephalography.

List of Acronyms III

T_1 T_1 relaxation time.

$T1w$ T_1 -Weighted.

T_2 T_2 relaxation time.

TLE Temporal Lobe Epilepsy.

TR Repetition Time.

$U-Net$ U-Shaped Convolutional Network.

WM White Matter.

XAI Explainable Artificial Intelligence.

Key References I

- [1] Patrick Kwan et al. "Definition of Drug Resistant Epilepsy: Consensus Proposal by the Ad Hoc Task Force of the ILAE Commission on Therapeutic Strategies". In: *Epilepsia* 51.6 (June 2010), pp. 1069–1077. ISSN: 1528-1167. DOI: 10.1111/j.1528-1167.2009.02397.x. PMID: 19889013.
- [2] Bushra Sultana et al. "Incidence and Prevalence of Drug-Resistant Epilepsy: A Systematic Review and Meta-analysis". In: *Neurology* 96.17 (Apr. 27, 2021), pp. 805–817. ISSN: 1526-632X. DOI: 10.1212/WNL.0000000000011839. PMID: 33722992.
- [3] S. Wiebe et al. "A Randomized, Controlled Trial of Surgery for Temporal-Lobe Epilepsy". In: *The New England Journal of Medicine* 345.5 (Aug. 2, 2001), pp. 311–318. ISSN: 0028-4793. DOI: 10.1056/NEJM200108023450501. PMID: 11484687.
- [4] Jiyao Sheng et al. "Drug-Resistant Epilepsy and Surgery". In: *Current Neuropharmacology* 16.1 (Jan. 2018), pp. 17–28. ISSN: 1570-159X. DOI: 10.2174/1570159X15666170504123316. PMID: 28474565. URL: <https://www.ncbi.nlm.nih.gov/pmc/articles/PMC5771378/> (visited on 06/20/2025).
- [5] Maurits W. Sanders et al. "Outcome of Epilepsy Surgery in MRI-Negative Patients Without Histopathologic Abnormalities in the Resected Tissue". In: *Neurology* 102.4 (Feb. 27, 2024), e208007. ISSN: 1526-632X. DOI: 10.1212/WNL.0000000000208007. PMID: 38290094.

Key References II

- [6] Daichi Sone. “Making the Invisible Visible: Advanced Neuroimaging Techniques in Focal Epilepsy”. In: *Frontiers in Neuroscience* 15 (2021), p. 699176. ISSN: 1662-4548. DOI: [10.3389/fnins.2021.699176](https://doi.org/10.3389/fnins.2021.699176). PMID: 34385902.
- [7] Seok-Jun Hong et al. “Automated Detection of Cortical Dysplasia Type II in MRI-negative Epilepsy”. In: *Neurology* 83.1 (July 1, 2014), pp. 48–55. ISSN: 1526-632X. DOI: [10.1212/WNL.0000000000000543](https://doi.org/10.1212/WNL.0000000000000543). PMID: 24898923.
- [8] Dan Ma et al. “Magnetic Resonance Fingerprinting”. In: *Nature* 495.7440 (Mar. 2013), pp. 187–192. ISSN: 1476-4687. DOI: [10.1038/nature11971](https://doi.org/10.1038/nature11971). PMID: 23486058. URL: <https://www.nature.com/articles/nature11971> (visited on 06/02/2025).
- [9] Zheng Ding et al. “Automated Whole-Brain Focal Cortical Dysplasia Detection Using MR Fingerprinting With Deep Learning”. In: *Neurology* 104.11 (June 10, 2025), e213691. ISSN: 1526-632X. DOI: [10.1212/WNL.000000000000213691](https://doi.org/10.1212/WNL.000000000000213691). PMID: 40378378.
- [10] Yin Yang et al. “Computational Modeling for Medical Data: From Data Collection to Knowledge Discovery”. In: *The Innovation Life* 2.3 (2024), p. 100079. ISSN: 2959-8761. DOI: [10.59717/j.xinn-life.2024.100079](https://doi.org/10.59717/j.xinn-life.2024.100079). URL: <https://www.the-innovation.org/article/doi/10.59717/j.xinn-life.2024.100079> (visited on 06/20/2025).

Key References III

- [11] Gary S. Collins et al. "Evaluation of Clinical Prediction Models (Part 1): From Development to External Validation". In: *BMJ (Clinical research ed.)* 384 (Jan. 8, 2024), e074819. ISSN: 1756-1833. DOI: [10.1136/bmj-2023-074819](https://doi.org/10.1136/bmj-2023-074819). PMID: 38191193.
- [12] Federico Cabitza et al. "The Importance of Being External. Methodological Insights for the External Validation of Machine Learning Models in Medicine". In: *Computer Methods and Programs in Biomedicine* 208 (Sept. 2021), p. 106288. ISSN: 1872-7565. DOI: [10.1016/j.cmpb.2021.106288](https://doi.org/10.1016/j.cmpb.2021.106288). PMID: 34352688.
- [13] Marzyeh Ghassemi, Luke Oakden-Rayner, and Andrew L. Beam. "The False Hope of Current Approaches to Explainable Artificial Intelligence in Health Care". In: *The Lancet. Digital Health* 3.11 (Nov. 2021), e745–e750. ISSN: 2589-7500. DOI: [10.1016/S2589-7500\(21\)00208-9](https://doi.org/10.1016/S2589-7500(21)00208-9). PMID: 34711379.
- [14] James L. Cross, Michael A. Choma, and John A. Onofrey. "Bias in Medical AI: Implications for Clinical Decision-Making". In: *PLOS digital health* 3.11 (Nov. 2024), e0000651. ISSN: 2767-3170. DOI: [10.1371/journal.pdig.0000651](https://doi.org/10.1371/journal.pdig.0000651). PMID: 39509461.
- [15] Katarzyna Borys et al. "Explainable AI in Medical Imaging: An Overview for Clinical Practitioners - Beyond Saliency-Based XAI Approaches". In: *European Journal of Radiology* 162 (May 2023), p. 110786. ISSN: 1872-7727. DOI: [10.1016/j.ejrad.2023.110786](https://doi.org/10.1016/j.ejrad.2023.110786). PMID: 36990051.

Key References IV

- [16] Ming Fan, Jiangning Song, and Zhaowen Qiu. “Editorial: Biomedical Image or Genomic Data Characterization and Radiogenomic/Image-Omics”. In: *Frontiers in Genetics* 13 (Aug. 17, 2022), p. 994880. ISSN: 1664-8021. DOI: 10.3389/fgene.2022.994880. PMID: 36061168. URL: <https://www.ncbi.nlm.nih.gov/pmc/articles/PMC9433120/> (visited on 06/20/2025).
- [17] Viktor Jirsa et al. “Personalised Virtual Brain Models in Epilepsy”. In: *The Lancet. Neurology* 22.5 (May 2023), pp. 443–454. ISSN: 1474-4465. DOI: 10.1016/S1474-4422(23)00008-X. PMID: 36972720.
- [18] Lohith G. Kini, James C. Gee, and Brian Litt. “Computational Analysis in Epilepsy Neuroimaging: A Survey of Features and Methods”. In: *NeuroImage. Clinical* 11 (2016), pp. 515–529. ISSN: 2213-1582. DOI: 10.1016/j.nicl.2016.02.013. PMID: 27114900.

Thank You Questions?